Rock and Soil Mechanics

Volume 43 | Issue 1 Article 7

3-23-2022

Dynamic prediction and influence factors analysis of ground surface settlement during tunnel excavation

Shuai JIANG
State Key Laboratory of Geomechanics and Geotechnical Engineering, Institute of Rock and Soil Mechanics, Chinese Academy of Sciences, Wuhan, Hubei 430071, China

Yong ZHU
University of Chinese Academy of Sciences, Beijing 100049, China

Qing LI
School of Architecture and Civil Engineering, Shenyang University of Technology, Shenyang , Liaoning 110870, China

Hui ZHOU
University of Chinese Academy of Sciences, Beijing 100049, China

See next page for additional authors

Custom Citation
JIANG Shuai, ZHU Yong, LI Qing, ZHOU Hui, TU Hong-liang, YANG Fan-jie, . Dynamic prediction and influence factors analysis of ground surface settlement during tunnel excavation[J]. Rock and Soil Mechanics, 2022, 43(1): 195-204.

Rock and Soil Mechanics 2022 43(1): 195−204
https: //doi.org/10.16285/j.rsm.2021.6201
ISSN 1000−7598
rocksoilmech.researchcommons.org/journal

Dynamic prediction and influence factors analysis of ground surface settlement during tunnel excavation

JIANG Shuai[1, 2], ZHU Yong[2, 3], LI Qing[1], ZHOU Hui[2, 3], TU Hong-liang[2, 3], YANG Fan-jie[2, 3]

1. School of Architecture and Civil Engineering, Shenyang University of Technology, Shenyang , Liaoning 110870, China
2. State Key Laboratory of Geomechanics and Geotechnical Engineering, Institute of Rock and Soil Mechanics, Chinese Academy of Sciences, Wuhan, Hubei 430071, China
3. University of Chinese Academy of Sciences, Beijing 100049, China

Abstract: The construction of urban subway tunnel inevitably produces disturbance to surrounding rock and causes ground surface settlement. Dynamic prediction of ground surface settlement caused by tunnel excavation is an important method to ensure the safety of above-ground buildings and tunnel construction. In view of the difficulty of accurate dynamic prediction of ground surface settlement during tunnel construction, based on the definition of longitudinal excavation coefficient γ, a dynamic prediction model of lateral ground surface settlement is established. The model can accurately describe the variation of the settlement of the same monitoring location with the advancement of the tunnel face, and then realize the dynamic prediction of the ground surface settlement at the construction site. The results show that under certain constraints, this model can be degenerated into Peck model and stochastic medium theory prediction model. The accuracy and applicability of the dynamic prediction model are verified by on-site construction. The tunnel can be divided into three affected segments longitudinally (i.e., intense influence, moderate influence, and mild influence) based on the obtained γ, which well reflected the influence degree of the excavated tunnel face on the same monitoring section at different positions. Through the analysis of the influence of the buildings and isolation piles on the ground surface settlement curve, it can be found that the building and its adjacent ground surface present the characteristics of cooperative deformation and joint bearing. Moreover, installing geological drill isolation piles on the side of the tunnel can reduce the ground surface settlement of that side up to 71.9%. The research results have a certain guiding and reference significance for the on-site construction of the Central Yunnan Water Diversion Project and similar projects.

Keywords: settlement prediction model; dynamic prediction; longitudinal excavation coefficient; stochastic medium theory; affected segmentation; on-site monitoring

1 Introduction

The construction of urban subway tunnel inevitably causes the deformation of the ground. The excavation of tunnel will produce disturbance to surrounding rock, which can cause surface settlement and deformation when transmitted to the surface. This in turn affects the normal use and structural safety of surface buildings, pavement structures and underground pipelines. Therefore, accurate prediction of surface settlement caused by tunnel excavation is very important to ensure the safety of surface buildings and tunnel construction.

Nowadays, many studies have been carried out on the deformation of the ground surface caused by tunnel excavation, and many important conclusions have been revealed. In general, the existing established models of surface settlement are all empirical formulas obtained by software fitting on the basis of a large number of actual monitoring data and considering the external factors affecting ground surface settlement[1−3]. At present, the most widely used methods for calculating ground surface settlement are as follows: Peck empirical formula[4] and stochastic medium theory method[5−7]. At the same time, many researchers have improved the two calculation methods in many aspects. Lu et al.[8] improved the Peck calculation model and obtained a new method to calculate the surface settlement caused by double-track subway tunnel excavation. Wu et al. [9], on the basis of analyzing the measured data of the surface settlement of shield tunnel in China, reversely deduced the value range of ground volume loss of shield tunnel with different diameters by using Peck formula. Zhu et al.[10] and O'Reilly et al.[11] analyzed the variation of some parameters such as the maximum surface settlement $S_{\max}$, the width of settlement tank i, and ground volume loss V_1. Based on the stochastic medium theory, Wang et al.[12] and Wei et al.[13] derived

Received: 3 August 2021 Revised: 10 September 2021
This work was supported by the National Natural Science Foundation of China (2019YFC0605104, 2019YFC0605103), the National Natural Science Foundation of China (41941018) and the Science and Technology Service Network Initiative of the Chinese Academy of Sciences (KFJ-STS-QYZD-174).
First author: JIANG Shuai, male, born in 1995, Postgraduate student, focusing on tunnel and underground space stability analysis. E-mail: 17854114851@163.com
Corresponding author: ZHOU Hui. male, born in 1972, PhD, Professor, Doctoral supervisor, research interests: rock mechanics test, theory, numerical analysis and engineering safety analysis., E-mail: hzhou@whrsm.ac.cn

some two-dimensional tunnel surface settlement prediction models for different environments. Han et al.[14] and Liu et al.[15] compared and analyzed the application conditions, theoretical connections and calculation results of Peck empirical formula method and stochastic medium theory method. They found that the surface settlement curve obtained by stochastic medium theory method has the same form as that by Peck empirical formula method. Through these exiting studies, it was found that most studies on the improvement of the Peck calculation model only considered the final ground surface deformation and did not pay attention to the dynamic variation of surface settlement in the same position with the advance of the tunnel face. In addition, many works of literature have pointed out that the settlement distribution curve obtained by stochastic medium theory method is similar to that obtained by Peck empirical formula method, so it is worth investigating whether the two calculation theories can be expressed in the same expression form.

At present, a lot of research have been done on the influence area division of the lateral ground surface settlement curve of tunnels[16−18]. However, there are few studies on the different settlements of ground monitoring points caused by excavation according to different positions of tunnels. The division of the affected segmentation of the tunnel longitudinally can be used to determine the position of the most unfavorable tunnel excavation sections of the monitoring points, which can provide a basis for timely adjustment of the excavation scheme and other reinforcement measures. Therefore, based on the Peck model, this paper introduces the longitudinal excavation coefficient γ, which can reflect the dynamic changes of the ground surface. Furthermore, the dynamic prediction model of ground surface settlement during tunnel excavation is established, and the constraint conditions are given to realize the degeneration of the dynamic model to the Peck calculation model and the stochastic medium theory model. On the basis of dynamic prediction model, the concept of the affected segmentation of longitudinal excavation is proposed, and the affected segmentation is divided according to the influence degree of tunnel excavation in different sections on the same monitoring cross section. Finally, the accuracy and applicability of the dynamic settlement prediction model are verified by on-site monitoring data and numerical calculation results. Meanwhile, the buildings and isolation piles affecting the ground surface settlement are also investigated. The research results have certain guiding and reference significance for the on-site construction of water diversion projects in Central Yunnan and similar projects.

2 Dynamic surface settlement prediction model and division of excavation affected segmentation considering longitudinal excavation coefficient

2.1 Peck empirical formula

Based on the analysis of a large number of monitoring data of surface settlement caused by tunnel excavation, Peck[4] believed that the transverse ground surface deformation during tunnel excavation was approximately Gaussian distribution, as shown in Fig. 1. W is the half of the total width of the surface settlement tank; $S_{\max}$ is the maximum settlement value corresponding to the surface settlement tank; α is the affected angle related to ground conditions; R is tunnel radius; and h is the depth from ground surface to tunnel center.

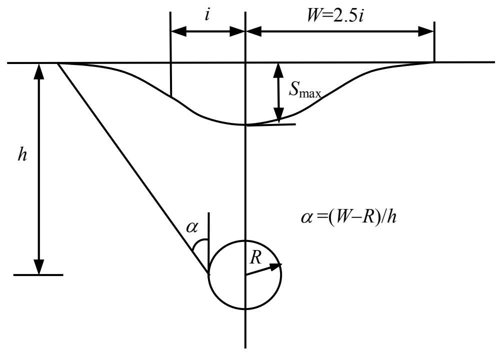

Fig. 1 Settlement tank distribution curve determined by Peck formula

Peck empirical formula of ground surface settlement caused by tunnel excavation is as follows:

$$S(x) = \frac{AV_1}{\sqrt{2\pi}i}\exp\left(-\frac{x^2}{2i^2}\right) \tag{1}$$

where x is the distance from the middle line of the tunnel; $S(x)$ is the surface settlement at the position x away from the tunnel axis; A is the cross-section area of the tunnel. The previous research [9] has studied the value of ground volume loss V_1 of tunnels with different diameters and concluded that the ground volume loss of tunnels with small and medium diameters was generally between 0% and 2.0%, and that of tunnels with large diameters was generally between 0% and 0.5%. For tunnels with small and medium diameters, the ground volume loss of tunnels decreases with the improvement of ground conditions.

In Eq. (1), i can be expressed as follows[11]:

$$i = Kh \tag{2}$$

where K is the parameter of the settlement tank width. For non-cohesive soil, the width parameter K is between 0.2 and 0.3. For stiff clay, the K value is between 0.4 and 0.5. For soft silty clay, it can be as

https://rocksoilmech.researchcommons.org/journal/vol43/iss1/7
DOI: 10.16285/j.rsm.2021.6201

high as 0.7.

2.2 Derivation of three-dimensional dynamic settlement prediction model for tunnel excavation

Equation (1) can only predict the final transverse settlement curve of the ground surface after tunnel excavation without considering the construction process. In actual engineering, however, the surface settlement curve of the same monitored position is constantly changing during the advance of the tunnel face. The three-dimensional map of the ground surface settlement caused by tunnel excavation is shown in Fig.2, where D is the tunnel diameter.

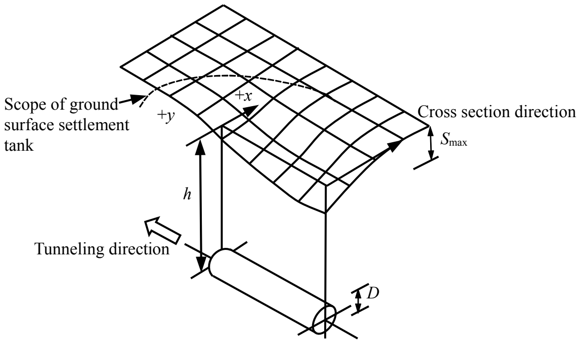

Fig. 2 Three-dimensional map of the ground surface settlement caused by tunnel excavation

In order to reflect the dynamic variation of the transverse settlement curve of the same ground surface monitoring section with the advance of the tunnel face, the longitudinal excavation coefficient, γ, which represents the influence of longitudinal excavation length on the settlement curve, was introduced based on Peck formula. It can be obtained:

$$S(x) = \gamma \frac{AV_1}{\sqrt{2\pi}i}\exp\left(-\frac{x^2}{2i^2}\right) \tag{3}$$

According to the stochastic medium theory, the rock and soil mass excavated can be regarded as numerous micro-cells of excavation, as shown in Fig.3. Then, the surface settlement deformation caused by tunnel excavation is the superposition of the influence of each excavation micro-cell on the surface.

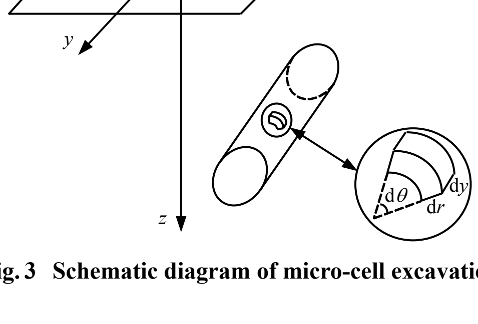

Fig. 3 Schematic diagram of micro-cell excavation

The surface settlement curve caused by tunnel excavation obtained by stochastic medium theory has the same distribution form as that obtained by Peck model[14–15]. The settlement along y direction caused by the excavation of micro-cells δ on the ground surface, Q_δ, was expressed in the form of Peck model, namely:

$$Q_\delta = \frac{V_\delta}{\sqrt{2\pi}j}\exp\left(-\frac{y^2}{2j^2}\right) \tag{4}$$

where y is the distance between the longitudinal monitoring position of the tunnel and the excavation micro-cell; V_δ is the ground volume loss being averaged to each micro-cell during tunnel excavation and unloading, and its value is related to some factors such as the ground conditions, tunnel excavation method, support and reinforcement method; and j is the width factor of tunnel longitudinal influence curve, and it can be expressed as

$$j = \lambda i = \lambda Kh \tag{5}$$

where λ is the scale coefficient of tunnel longitudinal width, which represents the relationship between the width of the transverse settlement tank i and the width factor of tunnel longitudinal j.

By integrating the surface settlement of excavation micro-cell in Eq. (4) within any excavation section (y_1, y_2) in the longitudinal direction of the tunnel, the longitudinal surface settlement $G(y_1, y_2)$ caused by excavation in this section can be obtained:

$$G_{(y_1,y_2)} = \int_{y_1}^{y_2}\int_0^{2\pi}\int_0^R Q_\delta r\mathrm{d}r\mathrm{d}\theta\mathrm{d}y \tag{6}$$

where y_1 is the distance between the tunnel face before tunnel excavation and the monitoring position; y_2 is the distance between the face at the end of longitudinal excavation and the monitoring position; r is the radius of tunnels; and θ is the rotation angle.

Substituting Eq. (4) into Eq. (6), we can get

$$G_{(y_1,y_2)} = \int_{y_1}^{y_2}\frac{V_\delta}{\sqrt{2\pi}j}\exp\left(-\frac{y^2}{2j^2}\right)\mathrm{d}y\int_0^{2\pi}\int_0^R r\mathrm{d}r\mathrm{d}\theta \tag{7}$$

When the tunnel is in the ultimate excavation condition (fully connected), the upper and lower limits of the longitudinal integral (y_1, y_2) are (–∞, +∞), and the corresponding surface settlement G_T is

$$G_T = \int_{-\infty}^{+\infty}\int_0^{2\pi}\int_0^R \frac{V_\delta}{\sqrt{2\pi}j}\exp\left(-\frac{y^2}{2j^2}\right)r\mathrm{d}r\mathrm{d}\theta\mathrm{d}y = V_\delta\int_0^{2\pi}\int_0^R r\mathrm{d}r\mathrm{d}\theta \tag{8}$$

The ratio of the settlement value of any longitudinal excavation interval (y_1, y_2) to the ultimate settlement value under the ultimate excavation condition is defined as the longitudinal excavation coefficient γ which can be expressed as

$$\gamma = \frac{\int_{y_1}^{y_2} \frac{V_\delta}{\sqrt{2\pi} j} \exp\left(-\frac{y^2}{2j^2}\right) \mathrm{d}y \int_0^{2\pi} \int_0^R r \mathrm{d}r \mathrm{d}\theta}{\int_{-\infty}^{+\infty} \frac{V_\delta}{\sqrt{2\pi} j} \exp\left(-\frac{y^2}{2j^2}\right) \mathrm{d}y \int_0^{2\pi} \int_0^R r \mathrm{d}r \mathrm{d}\theta} \tag{9}$$

Combining Eq. (8) and Eq. (9), we have

$$\gamma = \int_{y_1}^{y_2} \frac{1}{\sqrt{2\pi} j} \exp\left(-\frac{y^2}{2j^2}\right) \mathrm{d}y \tag{10}$$

By substituting Eq.(10) into Eq.(3), the dynamic settlement prediction model of the surface cross section of tunnel excavation is

$$S(x) = \frac{AV_1}{\sqrt{2\pi} i} \exp\left(-\frac{x^2}{2i^2}\right) \cdot \int_{y_1}^{y_2} \frac{1}{\sqrt{2\pi} j} \exp\left(-\frac{y^2}{2j^2}\right) \mathrm{d}y \tag{11}$$

where the physical significance of AV_1 is the convergence area (that is, the reduction of tunnel sectional area) after tunnel excavation.

2.3 Degeneration of dynamic prediction model to Peck model and 3D stochastic medium theory model

When the tunnel is in the ultimate excavation condition (fully connected), the upper and lower limits of the longitudinal integral (y_1, y_2) in Eq. (10) should be ($-\infty$, $+\infty$). At this time, the calculation result of longitudinal excavation coefficient γ is 1, and the dynamic prediction model in Eq. (11) degenerates into the classical Peck prediction model (Eq. (1)).

In Eq.(11), assuming that a micro tunnel is represented by a micro element $\mathrm{d}\xi\mathrm{d}\eta\mathrm{d}\varsigma$ (completely collapsed), the convergence area in the plane of tunnel section should be $\mathrm{d}\xi\mathrm{d}\eta$, as shown in Fig. 4. Taking the projection of the tunnel center on the ground as the coordinate origin, ξ and η in the figure are the coordinate positions of the micro-unit in the x and z directions relative to the coordinate origin. Ω is the tunnel section before the convergence; ω is the tunnel section after convergence, and AV_1 in Eq.(11) is replaced by the difference between the two areas. dy refers to the length of the excavation microcell in the y direction. If dy is represented by as $\mathrm{d}\varsigma$, which also represents the length of the excavation microcell in the y direction, it can be obtained

$$S(x) = \iint_{\Omega-\omega} \frac{1}{\sqrt{2\pi} i} \exp\left(-\frac{x^2}{2i^2}\right) \mathrm{d}\xi\mathrm{d}\eta \int_{y_1}^{y_2} \frac{1}{\sqrt{2\pi} j} \cdot \exp\left(-\frac{y^2}{2j^2}\right) \mathrm{d}\varsigma \tag{12}$$

It is assumed that the following conditions are true, that is

$$\sqrt{2\pi} i = \frac{z}{\tan\beta} \tag{13}$$

where z is the direction of tunnel depth; β is the main influence angle depending on ground conditions.

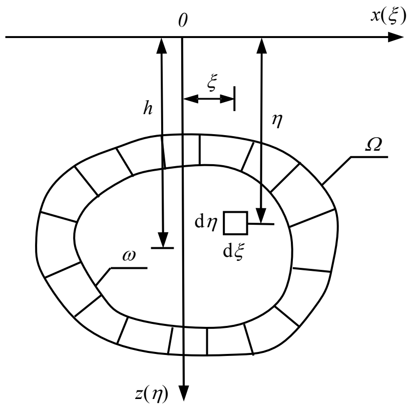

Fig. 4 Schematic diagram of excavation of any cross section of the tunnel

Under the condition of Eq. (13), Eq. (12) can be transformed into the following Eq. (14):

$$S(x) = \iint_{\Omega-\omega} \frac{\tan\beta}{z} \exp\left(-\frac{x^2 \pi \tan^2\beta}{z^2}\right) \mathrm{d}\xi\mathrm{d}\eta \cdot \int_{y_1}^{y_2} \frac{\tan\beta}{\lambda z} \exp\left(-\frac{y^2 \pi \tan^2\beta}{\lambda^2 z^2}\right) \mathrm{d}\varsigma \tag{14}$$

At this point, the form of Eq. (14) obtained is the same as the form of the prediction model of tunnel longitudinal settlement obtained by stochastic medium theory in literature[19]. However, the difference lies in that in the longitudinal direction, the dynamic prediction model in this work has one more correction coefficient λ than the calculation model in literature [19], which makes the model proposed in this paper closer to the on-site construction conditions. The main reason is that the disturbance to the face of the tunnel during the longitudinal excavation is different from that of the transverse surrounding rock. For example, a series of factors such as extrusion (shield construction) and excavation vibration make the longitudinal settlement and transverse settlement not exactly the same.

2.4 Inversion of dynamic settlement prediction model for tunnel excavation

According to Eq. (10), the longitudinal excavation coefficient γ is related to the distance y_1 between the tunnel face before excavation and the monitoring position, the distance y_2 between the tunnel face after excavation and the monitoring position, and the width factor j of the longitudinal influence curve. The width factor j of the longitudinal influence curve can be calculated by Eq.(5). In order to obtain the value of the scale coefficient λ of longitudinal width, this paper established numerical models of non-cohesive soil, stiff cohesive soil and soft cohesive soil, respectively, and adopted the three-step excavation method. The model size is shown in Fig.5. The settlement distribution curves of surface cross section were calculated when the longitudinal distance between the starting position of the tunnel face and the surface settlement monitoring section is 100, 15, 10, 5 and 0 m, respectively. When the distance between the starting position of the face and the surface settlement monitoring section is 100 m, the calculated longitudinal excavation coefficient γ is close to 1. Therefore, this condition can be considered as the maximum settlement condition of the monitored section (full excavation).

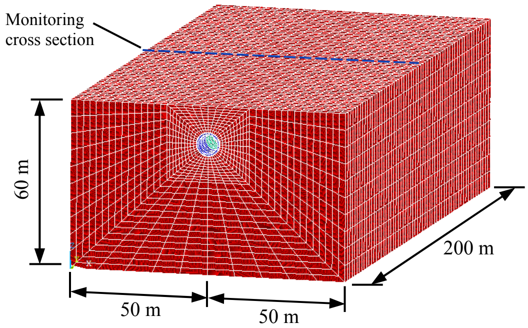

Fig. 5 Inversion calculation model

Based on the inversion of the distribution curve obtained by numerical simulation, the scale coefficient of longitudinal width λ is set as follows: 3.0 for silty clay, 0.9 for non-cohesive soil, and 0.9−3.0 for other soil. The better the ground conditions are, the smaller the ratio is.

Physical and mechanical parameters of each material are listed in Table 1.

Table 1 Physical and mechanical parameters of each material

Type	Density /(kg • m^{-3})	Elastic modulus /MPa	Poisson's ratio	Cohesion /kPa	Internal friction angle /(°)
Clay	1 860	11	0.35	34	10
Tunnel lining	2 602	3.0×10^4	0.20	—	—

The obtained transverse surface settlement curves at the same monitoring position under different excavation conditions are shown in Fig.6(a). In the cases of the width coefficient of settlement tank K=0.5, and the ground volume loss V_l=1.7%, the scale coefficient of longitudinal width obtained by inversion is equal to 1.2. The transverse surface settlement curves obtained by the dynamic settlement prediction model is shown in Fig. 6(b).

Figure 6 illustrates that the dynamic settlement curve determined by prediction model is in good agreement with that determined by numerical simulation, which indicates that the tunnel excavation dynamic prediction model has good applicability and accuracy, and also proves that the variation of the settlement curve obtained by the dynamic prediction model is more consistent with the actual situation. However, when the distance from the middle line of the tunnel is greater than 2.5i, the settlement value at the ground surface from the curve determined by the prediction model is close to 0, which has a certain error as compared with the numerical simulation results. This is mainly because the surface settlement curve from the prediction model is fitted according to the condition of Gaussian distribution, and the value of the Gaussian distribution function is approximately 0 when x >2.5i [20], which leads to the error between the calculated results and the actual monitoring data.

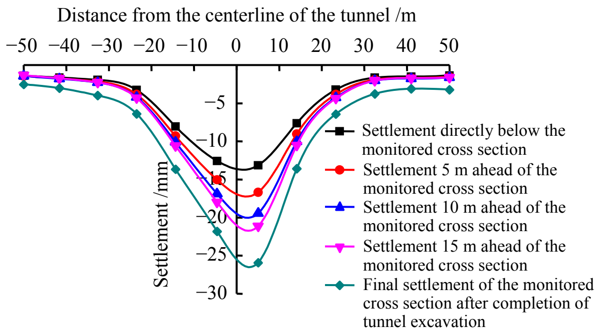

(b) Surface settlement curves calculated by numerical method

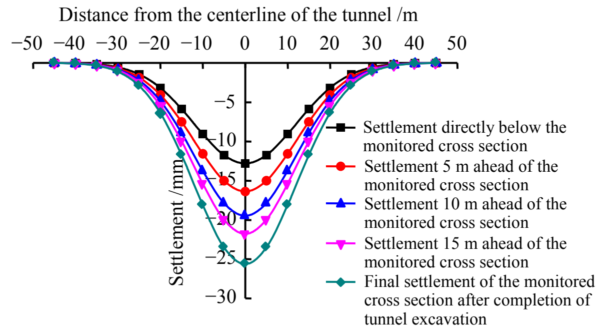

(b) Surface settlement curves calculated by dynamic prediction model

Fig. 6 Surface settlement curves at different distances between the starting point of tunnel excavation and the monitored cross section

2.5 Affected segmentation of tunnel longitudinal excavation

In order to meet the demand for monitoring range and provide basis for on-site monitoring, the concept of the affected segmentation of tunnel longitudinal excavation was proposed based on longitudinal excavation coefficient. According to the different settlement increment of the same surface monitoring section caused by excavation at different positions of the tunnel face of the excavation, the affected segmentation could be divided into three affected segmentations: the intensely affected segmentation of excavation, the moderately affected segmentation of excavation and the mildly affected segmentation of excavation. According to Eq. (10), the lateral monitoring section was taken as the center. In the longitudinal direction of the tunnel, γ is about 0.68 when the distance between the excavation tunnel face and the monitoring section is within 1.0 j. When the distance between the excavation tunnel face and the monitoring section is within 2.5 j, γ is about 0.99 [20]. This is used as the basis of tunnel longitudinal affected segmentation, and the final affected segmentation is divided as shown in Table 2.

Table 2 Division of longitudinal affected section of tunnel

Affected segmentation of tunnel	Range
Intensely affected segmentation	Tunnel longitudinal distance from monitoring section within the range of j
Moderately affected segmentation	Tunnel longitudinal distance from monitoring section in the range of j–$2.5j$
Mildly affected segmentation	Tunnel longitudinal distance from monitoring section beyond $2.5j$

As can be seen from Table 2, the division scope of the longitudinal excavation affected segmentation mainly depends on the width factor j of the longitudinal influence curve of the tunnel. According to Eq. (5), j is not only related to the buried depth h of the tunnel, but also related to surrounding rock conditions. The width coefficient of settlement tank K and the scale coefficient of longitudinal width λ differ under various surrounding rock conditions. The better the surrounding rock condition (the larger the internal friction angle φ), the smaller the K value and λ value. The lengths of the strongly affected segmentation and the moderately affected segmentation of tunnel excavation are therefore smaller.

3 Engineering application and validation

3.1 Project overview

Quaternary strata are distributed in the exit section of the Longquan tunnel in the water diversion of central Yunnan province. The strata from the surface down are artificial fill, red clay, gravel, and underlying limestone. The maximum buried depth of the simulated tunnel is 18.3 m, while the minimum buried depth is only 7.0 m. This tunnel passes through the soil layers, the soil-rock contact zone, and the rock layer in turn, as shown in Fig.7(a). As most parts of the tunnel studied are located near the soil-rock contact zone, the stability of the surrounding rock is very poor.

3.2 Monitoring programme

The length of the tunnel in the first excavation stage is 65 m. Four monitoring sections (monitoring section Ⅰ−Ⅰ, monitoring section Ⅱ−Ⅱ, monitoring section Ⅲ−Ⅲ and monitoring section Ⅳ−Ⅳ) and one monitoring point during construction (monitoring point V) were set up on site. The monitoring section Ⅳ−Ⅳ is located near the office building of Kunming Gas Company on the left (Fig. 7(b)), and the spacing between the other three monitoring sections is 10 m. The monitoring section Ⅰ−Ⅰ is 10 m away from the launch shaft. As shown in Fig.8, the monitoring point V during construction is located at the intersection of monitoring section Ⅱ−Ⅱ and tunnel axis.

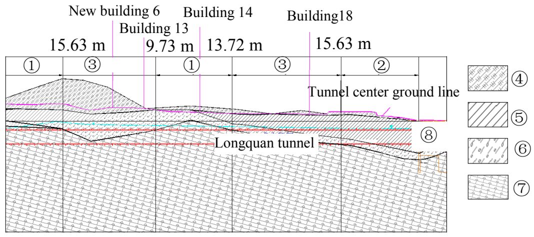

(a) Stratigraphic profile

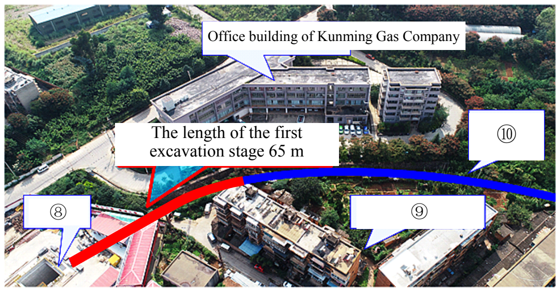

(b) Schematic diagram of the relative position of the tunnel passing by the building

① Rock stratum ② Soil layers ③ Upper soft and lower hard layer
④ Artificial fill ⑤Clay ⑥Gravelly soil ⑦Limestone ⑧ Launch shaft
⑨ Family community of Kunming Heavy Machine Tool Factory
⑩ Longquan tunnel exit section

Fig. 7 Construction site

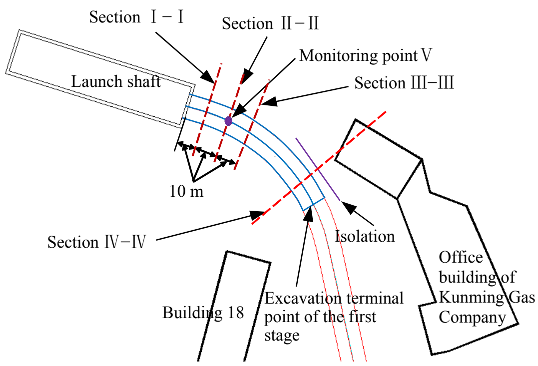

Fig. 8 Layout of monitoring points

3.3 Model mesh generation and material parameters setting

3.3.1 Model size and meshing

In order to eliminate the boundary effect of model, the width of the model is 100 m on the left and right sides of the tunnel axis, about 12 times the tunnel diameter (8.48 m). The longitudinal length of the tunnel is 300 m, and the starting point and end point of the tunnel are 50 m from the front and rear boundary of the strata boundary. In the direction of height, 100 m down from the bottom of the tunnel was taken, about 11 times the height of the tunnel (9.02 m), and the soil above the tunnel was taken as the actual buried depth of the tunnel. Since the damage caused by tunnel excavation is not considered, the buildings is equivalent to an elastic model with a certain mass. The numerical model constructed is presented in Fig. 9.

Three-step reserved core soil excavation method was adapted at construction site, and the left and right circulation footages were 1 m. Since the numerical simulation in this study only focused on the surface settlement, the excavation method was simplified as follows. The face of the three-step shape advanced in parallel, and the advance length of each step was 1 m. For the convenience of later analysis and comparison, the excavation of the interval tunnel is divided into three stages for analysis. The excavation in the first stage consisted of 65 excavation steps with a total of 65 m, and the second and third excavation stages were 45 m and 90 m.

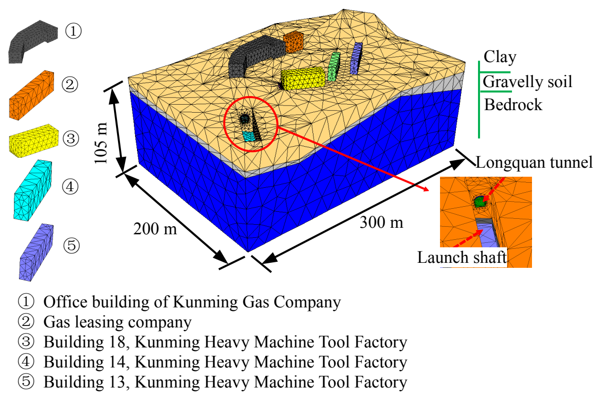

Fig. 9 Numerical calculation model

3.3.2 Setting model material parameters

In this study, the modified More-Coulomb constitutive model was selected. The primary support and secondary lining structure were established by using plate elements. The elastic modulus was determined according to the equivalent method[21], and the building weight was determined according to the *Load code for the design of building structures* (GB5009-2012)[22]. Physical and mechanical parameters of other materials were determined according to the monitoring reports, as shown in Table 3.

Table 3 Physical and mechanical parameters of each structural material

Type	Density /(kg • m^{-3})	Elastic modulus /MPa	Poisson's ratio
Primary support	2 602	2.72×10^4	0.20
Secondary lining	2 390	3.0×10^4	0.20
Building	500	2.33×10^4	0.30
Isolation pile	2 250	3.0×10^3	0.25

Physical and mechanical parameters of the soil layer determined according to geological survey data are listed in Table 4.

Table 4 Physical and mechanical parameters of soil layer

Type	Density /(kg • m^{-3})	Elastic modulus /MPa	Poisson's ratio	Cohesion /kPa	Internal friction angle /(°)
Clay	1 860	11	0.35	34	10
Gravelly soil	1 910	15	0.32	30	16
Limestone	2 610	180	0.24	851	45

3.4 Surface settlement curve during tunnel excavation

In order to verify the applicability of the method of affected segmentation of tunnel longitudinal excavation and the accuracy of numerical simulation results, the variation of the settlement value at monitoring position Ⅴ with tunneling was drawn, as shown in Fig. 10.

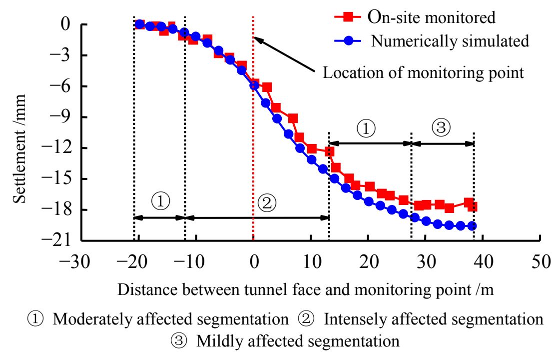

Fig. 10 Variation of ground surface settlement with the advancement of the tunnel face

The surface settlement firstly increased and then decreased in the process of tunneling. When the tunnel was excavated from 20 m in front of the monitoring point Ⅴ, the ground surface began to subside. With the increase of tunneling length, the rate of the settlement at the monitoring point continued to increase, and this rate reached the maximum when the tunnel face passed through the monitoring point. Passing through the monitoring section， tunnel face arrived at about 13 m, the settlement began to slow. The surface settlement tended to be stable when the tunnel face passed through the tunnel monitoring point for about 28 m. The curve of settlement over time is divided into three affected segmentations according to surface settlement rate, i.e. intensely affected segmentation, moderately affected segmentation, and mildly affected segmentation, which is consistent with the method of affected segmentation of tunnel longitudinal excavation described above. For the test segmentation, the numerical simulation result of the final settlement is slightly larger than the monitoring result of 1.9 mm. It can be demonstrated that the numerical simulation calculation result is basically consistent with the field monitoring result, thus proving the accuracy of the material parameters of the numerical model and its applicability to the subsequent tunnel excavation prediction.

3.5 Analysis of surface settlement curve

In order to verify the reliability of the dynamic settlement prediction model proposed in this paper, the settlement curves of monitoring section Ⅰ-Ⅰ−III-III during the first excavation stage were taken for comparison and analysis, as shown in Fig. 11. The monitoring section as was set as the starting position and the tunneling direction as the positive direction, the distances of the initial position and the end position of the tunnel face during the first excavation

Rock and Soil Mechanics, Vol. 43 [2022], Iss. 1, Art. 7

stage with respect to the monitoring section Ⅰ-Ⅰ are −10 m and 55 m, respectively. Therefore, the calculation interval of the corresponding dynamic settlement prediction model is (−10, 55). Similarly, the calculation intervals of the dynamic prediction model corresponding to the monitoring section Ⅱ-Ⅱ and monitoring section Ⅲ-Ⅲ are (−20, 45) and (−30, 35), respectively. As the tunnel is located near the soil-rock contact zone, the stratum condition is very poor. Therefore, the width scale coefficient of the dynamic prediction model λ is set as the maximum value of 3, the parameter of the settlement tank width K as 0.6, the ground volume loss V_1 as 0.9%, and the average buried depth as 13 m.

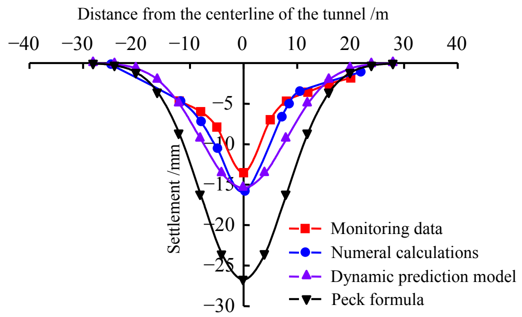

(a) Transverse ground surface settlement of Section Ⅰ-Ⅰ

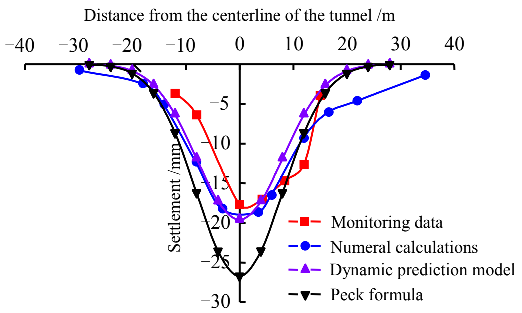

(b) Transverse ground surface settlement of Section Ⅱ-Ⅱ

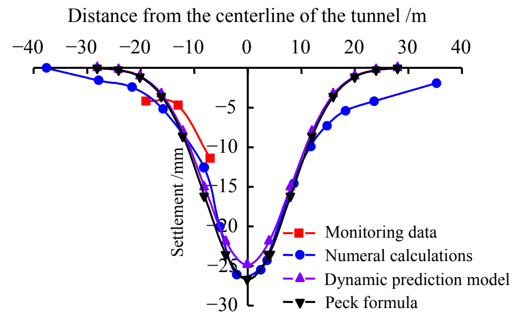

(c) Transverse ground surface settlement of Section Ⅲ-Ⅲ

Fig. 11 Transverse surface settlement curves of different monitoring sections

The results obtained from the three-dimensional dynamic prediction model for excavation settlement were compared with the measured settlement data on site and numerical calculation settlement results. It can be found from Fig.11 that the settlement curves obtained from the three methods were relatively consistent, which shows that the proposed settlement dynamic prediction model is reasonable, and it can be used to predict the dynamic surface settlement of the face of tunnel longitudinal excavation and monitoring face at different relative positions. The numerical simulation results presented that the surface settlement on the right side was larger than that on the left symmetric position when the distance from the tunnel centerline was more than 2 times the tunnel diameter. This was mainly because the excavated tunnel had a certain curvature, and during tunnel excavation, there was a phenomenon of disturbance concentration on the surrounding rock inside the curvature, which caused the cumulative disturbance to the surrounding rock on the right side of the tunnel to be greater than that on the left side. The specific principle is shown in Fig.12. When the position in the settlement curve obtained by the dynamic prediction model was more than 2.5i from the centerline of the tunnel, the predicted value of surface settlement was close to 0, which has a certain error with the results of numerical simulation and field monitoring. This is mainly due to the fact that γ was only about 0.01 when the tunnel face was excavated beyond the range of 2.5j from the monitoring section.

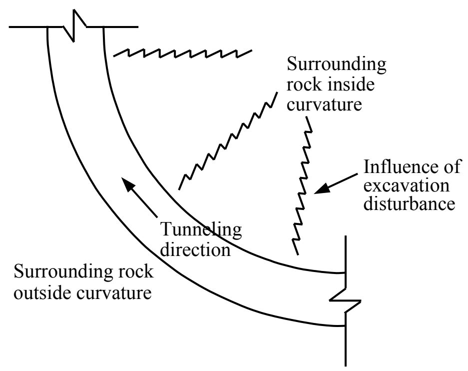

Fig. 12 Schematic diagram of surrounding rock disturbance on the inner side of tunnel excavation curvature

Compared with the results obtained by the Peck model, the settlement curve obtained by the dynamic prediction model shows a better consistency with the actual surface settlement curve. And the model can effectively reflect the variation of surface settlement caused by the change of monitoring section with the change of tunnel excavation position, thus achieving the purpose of dynamic prediction of surface settlement.

4 Influence of buildings and isolation piles reinforcement on the surface settlement curve

The dynamic settlement prediction model reflects the evolution of surface settlement in the process of tunnel construction. In addition, the factors affecting the shape of surface settlement curve include buildings and isolation piles. Relying on the actual engineering project, based on the settlement dynamic prediction model, this study further analyzes the influence of the buildings on one side of the tunnel and the application of isolation pile support on the surface settlement curve.

4.1 Characteristics of transverse surface settlement curve near buildings

When the tunnel passes through the building at close range, the transverse settlement curve at this location is bound to be affected by buildings. Buildings in an actual engineering site were used for analysis to explore the influence of buildings on the lateral surface settlement curve. The building is 9.43 m away from the edge of the tunnel. Figure 13 shows the comparison of surface settlement curves of monitoring section Ⅳ-Ⅳ caused by tunnel lateral excavation under three different working conditions, i.e. without no buildings, with buildings and 50% reduction of elastic modulus of building.

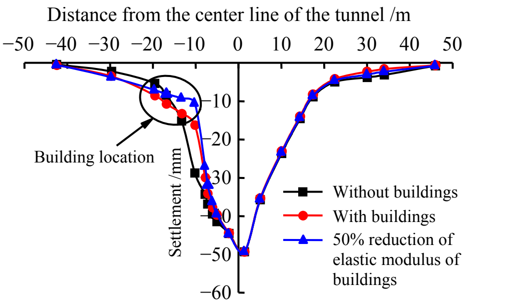

(a) Transverse surface settlement curve in the first excavation stage

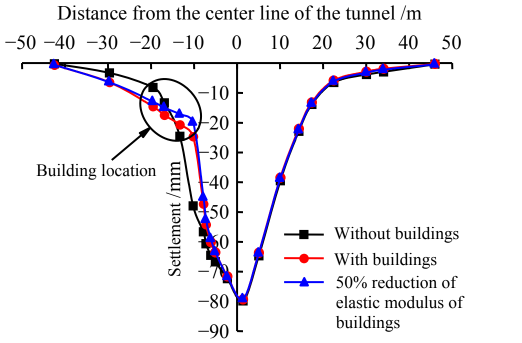

(b) Transverse surface settlement curve in the second excavation stage

Fig. 13 Comparison of surface settlement of section Ⅳ-Ⅳ under different building conditions

It can be observed from Fig.13 that compared with the working condition without buildings, the reduction of surface settlement of monitoring section Ⅳ-Ⅳ is 44% and 63%, respectively in the first excavation stage and the two working conditions with buildings and 50% reduction of elastic modulus of buildings, meanwhile the increase of surface settlement on the side of buildings away from the tunnel is 59% and 34%, respectively. Similarly, in the second excavation stage, under these two working conditions, the reduction of surface settlement of monitoring section Ⅳ-Ⅳ is 49% and 58%, respectively, while the increase of surface settlement on the side of buildings away from the tunnel is 78% and 59%, respectively. The existence of buildings makes the surface curve gentle, which is mainly due to the local increase of the surface stiffness at the building, resulting in the coordinated deformation of the building and its adjacent surface to bear the load together.

In addition, the influence of building material parameters on surface settlement was weakened when the tunnel was excavated at a longer distance from monitoring section Ⅳ-Ⅳ. The influence of buildings on the surface settlement curve was mainly on the side near the building, and that on the other side of the tunnel and the position directly above the excavated tunnel was very weak.

4.2 Characteristics of lateral surface settlement curve after isolation pile reinforcement

Two rows of isolation piles in the form of quincunx arrangement were applied between the office building of Kunming Gas Company and the tunnel for simulation analysis. There are 65 isolation piles in total, with a diameter of 200 mm and a length of 3 m into the rock. The layout of isolation piles is shown in Fig.14.

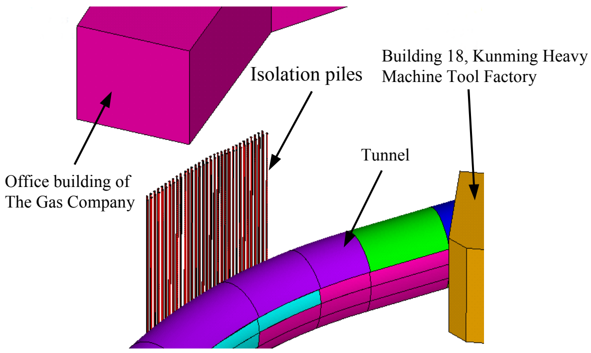

Fig. 14 Layout of isolation pile

The surface settlement curves of monitoring section Ⅳ-Ⅳ under the condition of isolation pile in the first excavation stage and the subsequent excavation stage were selected in order to analyze the influence of isolation pile reinforcement on the surface settlement curve, as shown in Fig.15.

The results shown in Fig.15 are consistent with the findings in the existing literature[23]. The maximum surface settlement of the tunnel with a small turning radius is no longer located directly above the arch crown but tends to the right side of the tunnel center line (i.e., inside the curvature) within the radius of one time of the tunnel diameter. By comparing the two working conditions with and without isolation piles, it can be found that for the monitored section Ⅳ-Ⅳ in the second excavation stage and the third excavation stage under the working condition of applying isolation piles, the maximum settlement was reduced by 14.78 mm and 15.36 mm, with the reduction ratio of 71.9% and 71.1%, respectively. Hence, it is concluded that the installation of isolation piles has an obvious isolation effect on the surface settlement of the arch crown of monitored section Ⅳ-Ⅳ. The excavation in the first stage led to the largest settlement of the monitored section, and the influence of the subsequent excavation on the surface settlement gradually weakened with the increase of the distance from the monitored section.

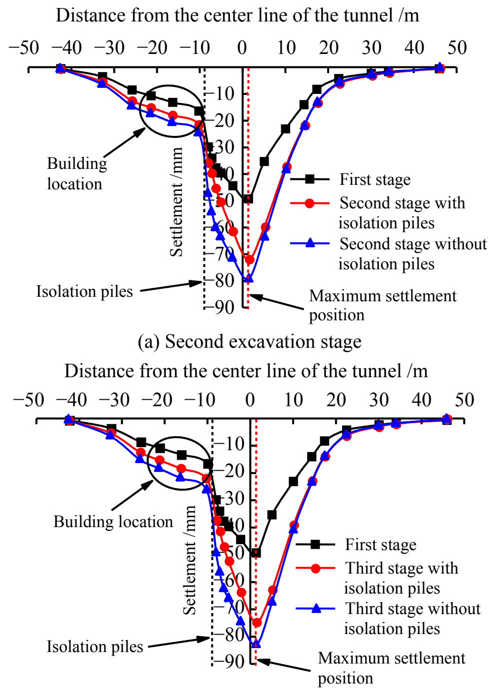

(a) Second excavation stage

(b) Third excavation stage

Fig. 15 Comparison of surface settlement of section Ⅳ-Ⅳ under different isolation pile conditions

5 Conclusions

(1) A set of dynamic prediction model of surface settlement suitable for tunnel excavation was proposed. Based on the Peck empirical formula, the model introduced the longitudinal excavation coefficient to characterize the variation of the surface settlement curve at the same position affected by the change of the position of the tunnel face, and the model can accurately achieve the purpose of real-time prediction of dynamic tunnel excavation.

(2) By imposing some specific constraint conditions, the settlement dynamic prediction model can degenerate to the Peck model and the stochastic medium theory model.

(3) The concept of longitudinal excavation affected segmentation was introduced in the longitudinal direction of the tunnel to characterize the influence degree of the longitudinal excavation section of the tunnel on a transverse surface settlement. Based on the longitudinal excavation coefficient, the tunnel is longitudinally divided into intensely affected segmentation, moderately affected segmentation and mildly affected segmentation, which can provide the basis for in-situ excavation and monitoring work.

(4) The influence of buildings on the transverse surface settlement curve is as follows: the existence of buildings flattens the surface settlement curve, and the buildings and the surrounding strata show cooperative deformation and common bearing characteristics. The surface settlement curve is mainly affected by the buildings close to the side of the tunnel, and the curve on the other side and the surface settlement directly above the tunnel center line are slightly affected.

(5) Due to the control effect of isolation piles on the ground deformation, in the transverse surface settlement curve, the settlement values of the side imposed by the isolation pile decreased. The existence of isolation piles reduced the surface settlement at the position of isolation piles by 71.9% and 71.1% in the second excavation stage and the third excavation stage, respectively.

References

[1] JIN D L, YUAN D J, LI X G, et al. Analysis of the settlement of an existing tunnel induced by shield tunneling underneath[J]. Tunnelling and Underground Space Technology, 2018, 81(11): 209−220.

[2] FU J Y, YANG J S, ZHANG X M, et al. Response of the ground and adjacent buildings due to tunnelling in completely weathered granitic soil[J]. Tunnelling and Underground Space Technology, 2014, 43(7): 377−388.

[3] LI Fang-ming, CHEN Guo-xing. Study on deformation characteristics of ground surface settlement during shield tunnel construction of river floodplain in Nanjing[J]. Journal of the China Railway Society, 2020, 42(7): 155−160.

[4] PECK R B. Deep excavations and tunneling in soft ground[C]//Proceedings of 7th International Conference of Soil Mechanics and Foundation Engineering. Mexico City: [s. n.], 1969: 225−290.

[5] ZENG Bin, HUANG Da, PENG Nian, et al. Analogous stochastic medium theory method(ASMTM) for predicting soil displacement induced by general and special-section shield tunnel construction[J]. Chinese Journal of Rock Mechanics and Engineering, 2018, 37(Suppl. 2): 4356−4366.

[6] LITWINSZYN J. The theories and model research of movements of ground masses[C]//Proceedings of the European Congress Ground Movement. Leeds: [s. n.], 1957: 202−209.

[7] FU He-lin, LI Jie, WANG Hong-tao, et al. Research on the ground settlement prediction in shallow tunnel under unsymmetrical pressure based on stochastic medium theory[J]. Journal of Railway Engineering Society, 2017, 34(9): 70−76.

[8] LU Jian, YAO Ai-jun, ZHENG Xuan, et al. Study on the law and computational method of ground surface settlement induced by double-line tunnel excavation[J]. Chinese Journal of Rock Mechanics and Engineering, 2019, 38(Suppl. 2): 3735−3747.

[9] WU Chang-sheng, ZHU Zhi-duo. Comparative study on ground loss ratio due to shield tunnel with different diameters[J]. Chinese Journal of Geotechnical Engineering, 2018, 40(12): 2257−2265.

[10] ZHU Cai-hui, LI Ning. Estimation method and laws analysis of surface settlement due to tunneling[J]. Rock and Soil Mechanics, 2016, 37(Suppl. 2): 533−542.

[11] O'REILLY M P, NEW B M. Settlements above tunnels in the United Kingdom—their magnitude and prediction[C]// Proceedings of Tunnelling 82. London: Institution of Mining and Metallurgy, 1982: 173−181.

[12] WANG X D, TAN W J, Ni P P, et al. Propagation of settlement in soft soils induced by tunneling[J]. Tunnelling and Underground Space Technology, 2020, 99: 103378.

[13] WEI Gang, ZHOU Yang-kan. A simplified method for predicting ground settlement caused by adjacent parallel twin shield tunnel construction based on stochastic medium theory[J]. Rock and Soil Mechanics, 2016, 37(Suppl. 2): 113−119.

[14] HAN Xuan, LI Ning. Comparative analysis of strata prediction models for ground movement induced by tunnel construction[J]. Chinese Journal of Rock Mechanics and Engineering, 2007, 26(3): 594−600.

[15] LIU Bo, TAO Long-guang, YE Sheng-guo, et al. Back analysis prediction system for ground deformation due to subway tunneling excavation[J]. Journal of China University of Mining & Technology, 2004, 33(3): 227−282.

[16] YI Li. Study on the influence zoning of the new urban tunnel under the existing road[J]. Chinese Journal of Underground Space and Engineering, 2020, 16(5): 1490−1497.

[17] YANG Xiao-long, FANG You-liang, LÜ Zhi-zhou. Surface settlement prediction and impact zone division for double tube tunnel in Kunming soft soil area[J]. Modern Tunneling Technology, 2019, 56(Suppl. 2): 347−354.

[18] QIU Wen-ge, SUN Ke-guo, ZHENG Qiang, et al. Study on influence division of fill and excavation above tunnel by the initial depth[J]. China Civil Engineering Journal, 2017, 50(Suppl. 1): 8−13.

[19] SHI Cheng-hua, PENG Li-min. Application of stochastic medium theory to predicting settlement in longitudinal surface due to tunnel construction by shield[J]. Rock and Soil Mechanics, 2004, 25(2): 320−323.

[20] SHENG Zhou, XIE Shi-qian, PAN Cheng-yi. Probability and mathematical statistics[M]. Beijing: Higher Education Press, 2020.

[21] LI Chun-qing, LIANG Qing-guo, WU Xu-yang, et al. Analysis on rigidity of primary support of composite lining and its influencing factors[J]. Tunnel Construction, 2014, 34(8): 754−759.

[22] Ministry of Housing and Urban-Rural Development of the People's Republic of China. GB 50009－2012 Load code for the design of building structures[S]. Beijing: China Building Industry Press, 2012.

[23] DENG Huang-shi, FU He-lin, SHI Yue. Calculation of surface settlement caused by excavation of shield tunnels with small turning radius[J]. Chinese Journal of Geotechnical Engineering, 2021, 43(1): 165−173.